

N72-29866

NATIONAL AERONAUTICS AND SPACE ADMINISTRATION

Technical Memorandum 33-556

*Scan Pointing Calibration for the
Mariner Mars 1971 Spacecraft*

W. F. Havens

G. I. Jarvin

G. D. Pace

R. A. Virzi

**CASE FILE
COPY**

**JET PROPULSION LABORATORY
CALIFORNIA INSTITUTE OF TECHNOLOGY
PASADENA, CALIFORNIA**

August 1, 1972

NATIONAL AERONAUTICS AND SPACE ADMINISTRATION

Technical Memorandum 33-556

*Scan Pointing Calibration for the
Mariner Mars 1971 Spacecraft*

W. F. Havens

G. I. Jaivin

G. D. Pace

R. A. Virzi

JET PROPULSION LABORATORY
CALIFORNIA INSTITUTE OF TECHNOLOGY
PASADENA, CALIFORNIA

August 1, 1972

PREFACE

The work described in this report was performed by the
Guidance and Control Division of the Jet Propulsion
Laboratory, under the cognizance of the Mariner Mars
1971 Project

Page Intentionally Left Blank

CONTENTS

I.	Introduction	1
II.	Scan Pointing System	2
III.	Coordinate Systems and Error Model	5
IV.	Scan Ground Calibration	9
V.	Scan In-Flight Calibration	21
VI.	Results and Conclusions	32
Appendix A.	Results of Scan I	35
Appendix B.	Results of Scan II	38
References	41

TABLES

1.	Attitude control and scan telemetry measurements	9
2.	Control loop potentiometer calibration accuracy	12
3.	Ground calibration offset values	18
4.	Ground calibration results	20
5.	In-flight calibration results	32
6.	Scan pointing accuracy	33

FIGURES

1.	Mariner Mars 1971 spacecraft	3
2.	Scan control subsystem (single axis)	4
3.	Clock and cone angles	5
4.	Platform LMN coordinates	6
5.	Scan pointing angular offsets	8
6.	Scan ground calibration and alignment diagram	10
7.	Control loop calibration corrections	14
8.	Platform offsets	15
9.	Spacecraft offsets	16

CONTENTS (contd)

FIGURES (contd)

10.	Residual roll null offset	19
11.	Scan in-flight calibration software data flow	23
12.	Simulated and actual TV star picture	25
13.	Video contour plot of 6.9 magnitude star	26
14.	Search pattern for Scan I	27
15.	Search pattern for Pleiades pictures	28
16.	Scan II sequence	30

ABSTRACT

The methods used to calibrate the pointing direction of the M'71 spacecraft scan platform are described here. Accurate calibration was required to meet the pointing accuracy requirements of the scientific instruments mounted on the platform. A detailed ground calibration was combined with an in-flight calibration utilizing narrow angle television pictures of stars. Results of these calibrations are summarized.

SECTION I

INTRODUCTION

A two-degree-of-freedom gimballed scan platform was utilized to point the Mariner '71 science instruments. Accurate calibration of platform pointing was required to meet the scientific requirements of the mission. An a priori pointing control accuracy of 0.5° (3σ) and a posteriori knowledge of where the platform had pointed of 0.25° (3σ) was desired by the Mariner '71 mission.

Experience gained on M'69 dictated that a new calibration technique be employed to improve accuracy. Calibration on M'69 was obtained by taking numerous electrical and mechanical measurements with the spacecraft in a full system configuration. This required considerable effort and consumed much system testing time. Accuracy was limited by the test configuration and instrumentation. In particular, the scan actuators could not support the platform weight in a 1 g field. The test setup devised to support the platform introduced mechanical distortions in the spacecraft and platform structure on the order of the biases being measured.

To overcome these drawbacks, a two-part calibration scheme was devised for M'71. The first part consisted of a ground calibration which combined analytically the separate calibration of the scan pointing elements. This allowed calibration to proceed simultaneously among several subsystems independently. System test time was reduced by limiting system testing to the determination of subsystem electro-mechanical interactions and the verification of analyses. The second part of the calibration consisted of an in-flight calibration utilizing narrow angle television pictures of stars. This provided the end-to-end system calibration with an accuracy sufficient to assure that mission pointing requirements could be met.

SECTION II

SCAN POINTING SYSTEM

Pointing of the platform relative to the spacecraft is accomplished by articulating the platform about its two control axes, clock and cone. A three-axis stabilized spacecraft orientation is maintained by a cold gas reaction control system utilizing celestial sensor error signals. Sun sensors measure rotations about two axes, pitch and yaw, while a Canopus sensor measures rotations about the third control axis, roll. A view of the spacecraft and platform is shown in Figure 1.

A simplified representation of one axis of the scan control subsystem is shown in Figure 2. On board (CC&S) or ground (QC) commands are received to step the platform in 0.25° increments. A stepper motor moves the wiper on a reference potentiometer to create a reference voltage. When the reference pot is selected, the analog servo loop responds until the feedback voltage, as measured by the feedback potentiometer, cancels the reference voltage. A preset reference pot whose output value is set prior to launch is also available as a reference. A ground command is available to select which pot is to be used. Additional details on the attitude control and scan subsystems may be found in Reference 1.

Numerous telemetry (T/M) measurements are available to assess attitude control and scan control performance. Analog measurements are quantized into 7-bit digital telemetry words. Thus, each measurement has a value expressed in data number (DN) of from 0 to 127. Telemetry measurements from the celestial sensors provide attitude control position information. Potentiometers geared to the gimbals provide coarse and fine scan telemetry measurements. The fine measurement is shared with a measurement of the reference potentiometer setting. The fine telemetry is available only when scan power is on.

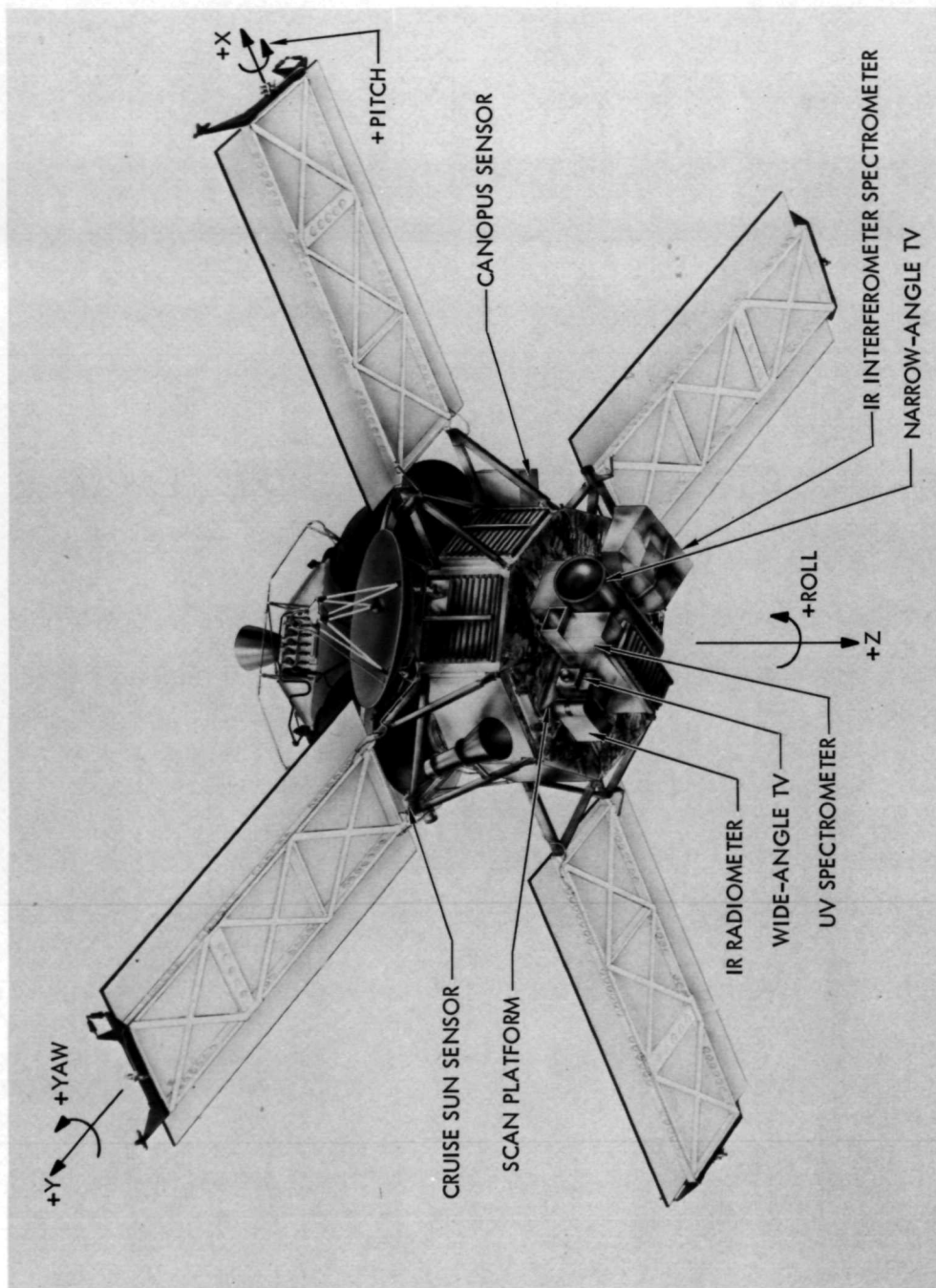


Figure 1. Mariner Mars 1971 Spacecraft

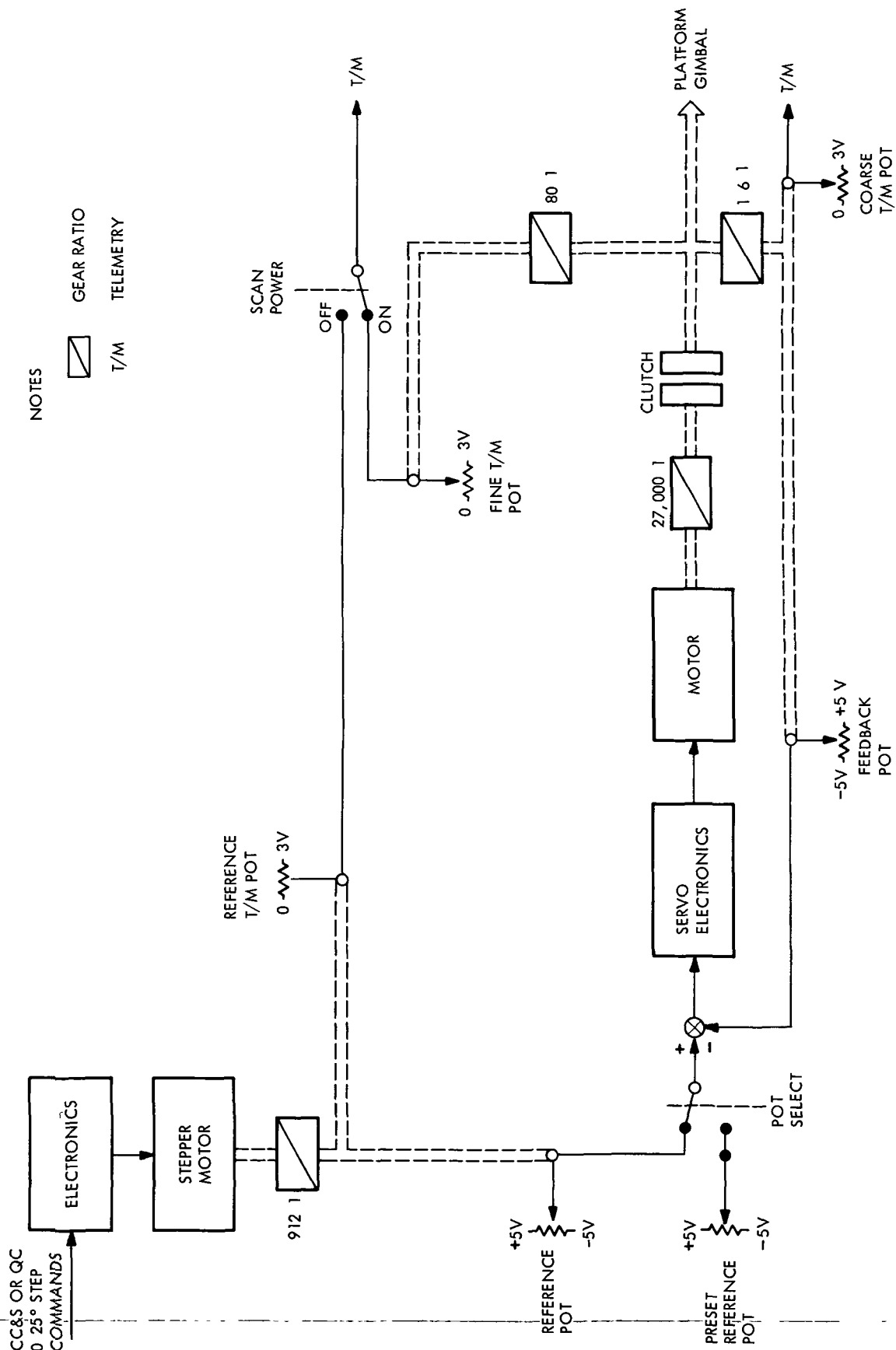


Figure 2. Scan Control Subsystem (Single Axis)

SECTION III

COORDINATE SYSTEMS AND ERROR MODEL

Spacecraft Clock and Cone Coordinates

Pointing direction to a body from the spacecraft is specified by the clock and cone angles as defined in Figure 3. The relationship between these angles and the spacecraft pitch, yaw, and roll axes is shown also. Figure 1 illustrated the orientation of the pitch, yaw, and roll axes in the spacecraft frame. The cone angle of an object is the angle, β (where $0 \leq \beta \leq 180^\circ$), from the spacecraft-sun line to the spacecraft-object line. The clock angle of an object is the angle, α (where $0 \leq \alpha \leq 360^\circ$), between a plane containing the sun, spacecraft, and Canopus and a plane containing the sun, spacecraft and object, and is measured from the sun-spacecraft-Canopus plane in the clockwise direction when looking toward the sun from the spacecraft. Platform motion is mechanically limited to 90° to 305° in clock and 96° to 165° in cone.

\vec{S} = VECTOR TO CANOPUS
 \vec{C} = VECTOR TO SUN
 $\vec{B} = \vec{C} \times \vec{S} / |\vec{C} \times \vec{S}|$
 $\vec{A} = \vec{B} \times \vec{C}$ (PLANE $\vec{A}\vec{C}$ CONTAINS \vec{S})

α = CLOCK ANGLE
 β = CONE ANGLE

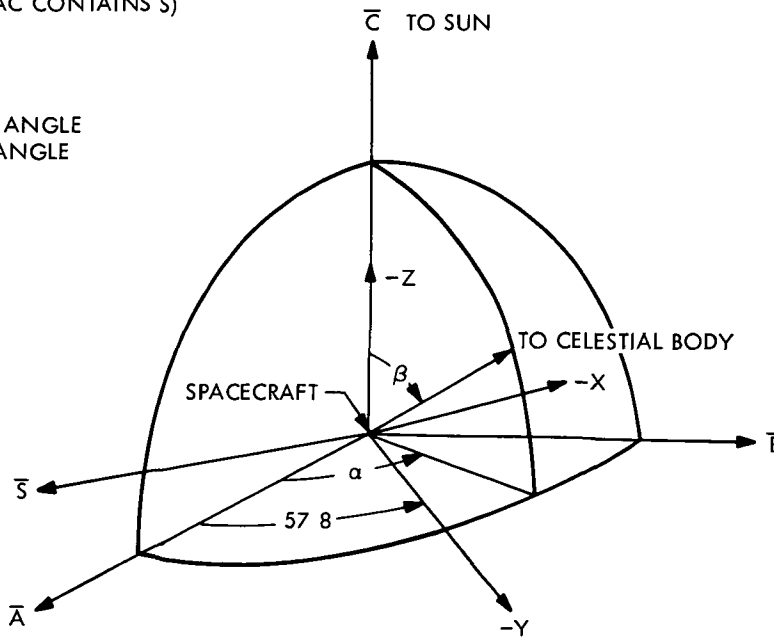


Figure 3 Clock and Cone Angles

Platform Coordinates

Relative pointing directions of instruments on the platform are defined using a set of right-handed cartesian unit vectors, LMN. For calibration purposes the L vector was chosen as the line-of-sight through the central reseau of the vidicon of the narrow angle television (TV-B). Offsets of other instruments were referenced to TV-B. The relationship between the LMN system and the clock-cone system is illustrated in Figure 4.

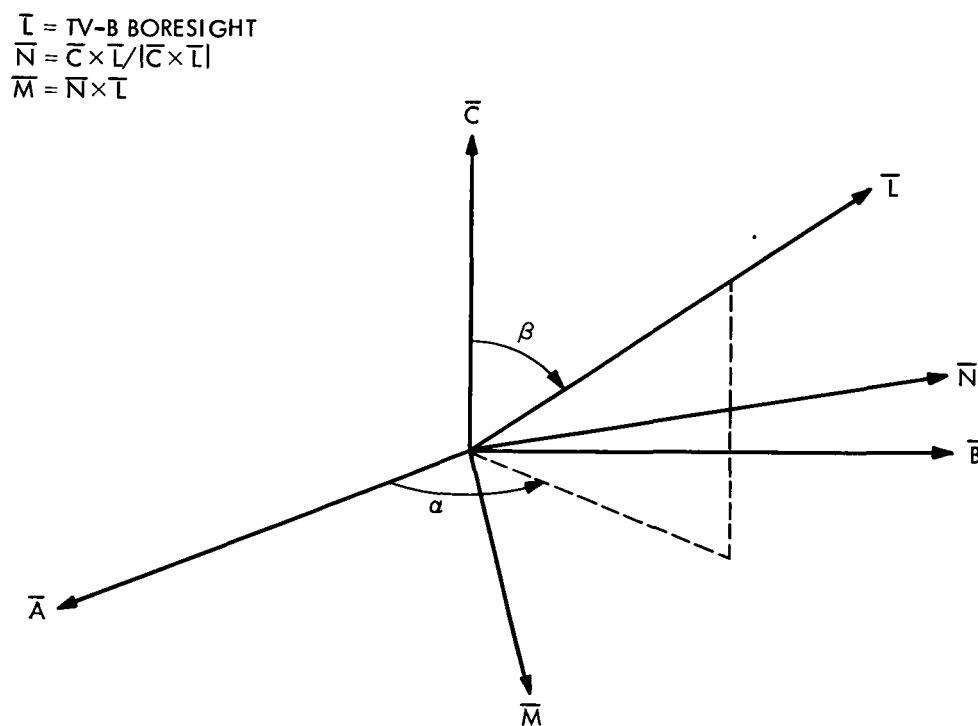


Figure 4. Platform LMN Coordinates

Error Model

Misalignments and null offsets in the various scan pointing elements will cause overall pointing errors. Equations (1) through (3) give the true pointing direction in the presence of these errors.

$$\alpha = \alpha_G + \chi / \sin \beta_G \quad (1)$$

$$\beta = \beta_G + \Psi \quad (2)$$

$$\tau = \rho - \chi \cot \beta_G \quad (3)$$

α and β are the true clock and cone pointing direction. The twist angle, τ , is a right-handed rotation of the TV field-of-view about its line-of-sight. The angles α_G and β_G are the platform gimbals clock and cone angles assuming no errors. All errors are lumped into the three orthogonal small rotations Ψ , χ , and ρ , the cone offset, cross-cone offset and rotation offset angle, respectively.

The offset angles are comprised of eight generalized error rotations as given in equations (4) through (6)

$$\Psi = \theta_1 - \theta_6 \sin \alpha_G + \theta_7 \cos \alpha_G \quad (4)$$

$$\chi = \theta_2 + \left[\theta_4 + \theta_8 \cot \beta_S \right] \sin \beta_G - \left[\theta_5 + \theta_6 \cos \alpha_G + \theta_7 \sin \alpha_G \right] \cos \beta_G \quad (5)$$

$$\rho = \theta_3 + \left[\theta_4 + \theta_8 \cot \beta_S \right] \cos \beta_G + \left[\theta_5 + \theta_6 \cos \alpha_G + \theta_7 \sin \alpha_G \right] \sin \beta_G \quad (6)$$

These error rotations are illustrated in Figure 5. β_S is the Canopus cone angle. Not shown is θ_8 , the Canopus sensor non-orthogonality. All known error sources can be lumped into these eight basic rotations.

Equations (1) through (6) represent the error model used throughout the ground and in-flight calibrations. They were used to evaluate known rotations such as fixed mechanical offsets and limit cycle motion. In addition, they were used to evaluate overall pointing accuracy due to uncertainties.

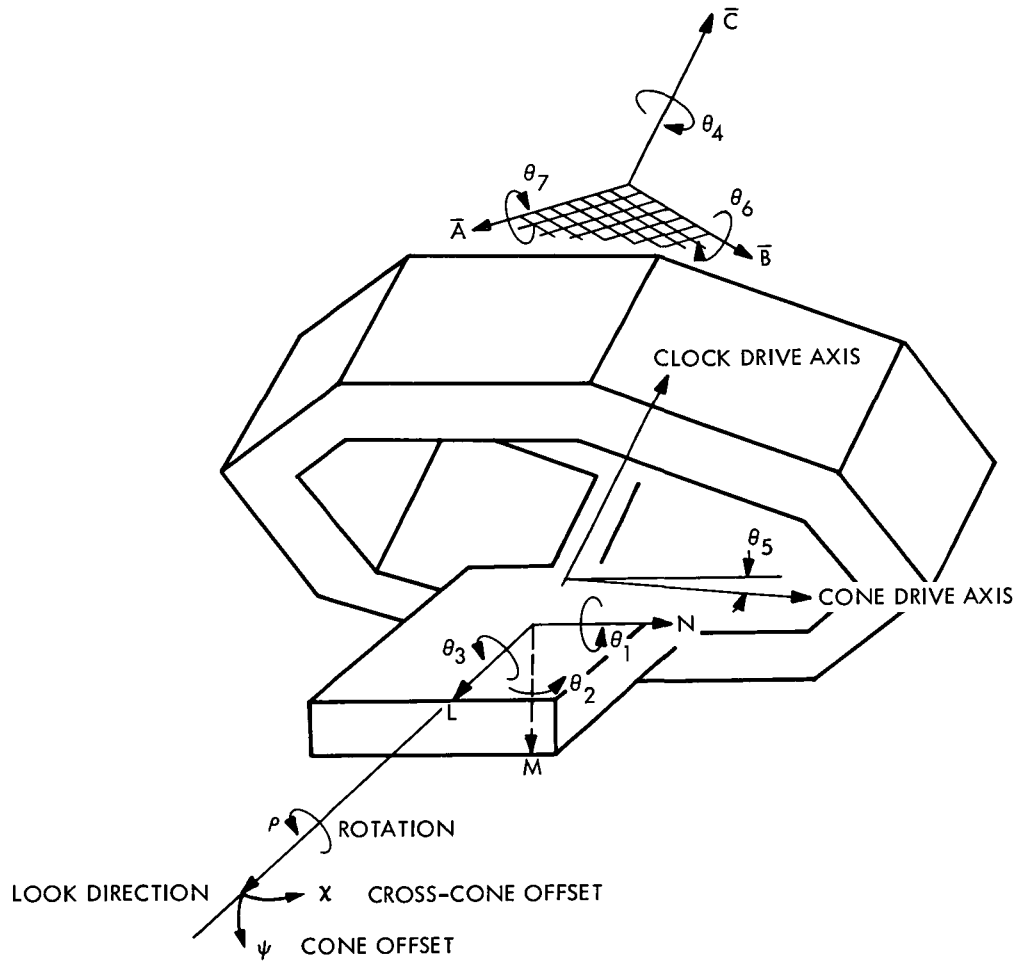


Figure 5. Scan Pointing Angular Offsets

SECTION IV

SCAN GROUND CALIBRATION

A comprehensive ground calibration was developed (References 2 and 3) to obtain initial estimates of offsets and calibrations not available from the subsequent in-flight calibration. The subsystems and elements involved in the calibration are illustrated in Figure 6. The plan developed consisted of a telemetry calibration, a control loop calibration and calibration of the fixed mechanical offsets. Although ground calibration data was obtained for the proof test model (PTM) and the two flight spacecraft, only data for Mariner 9 is given here.

Telemetry Calibration

Calibrations of the scan and attitude control telemetry defined in Table 1 are summarized in Reference 4. Table 1 gives the resolution of each measurement and the calibration accuracy achieved. Note that the calibration accuracies obtained were better than the resolution with the exception of the scan cone and clock fine position.

Table 1. Attitude Control and Scan Telemetry Measurements

Channel	Measurement	Resolution Degrees/DN	3 σ Accuracy Degrees
105/112	Pitch sun sensor fine/coarse position	0.015/0.04	0.006/0.006
106/113	Yaw sun sensor fine/coarse position	0.015/0.04	0.006/0.006
107/114	Roll Canopus sensor fine/coarse position	0.03/0.06	0.014/0.02
200	Scan clock coarse position	1.75	0.2
201	Scan cone coarse position	1.75	0.2
207	Scan cone fine position/reference pot	0.035/1.75	0.06/0.2
227	Scan clock fine position/reference pot	0.035/1.75	0.06/0.2

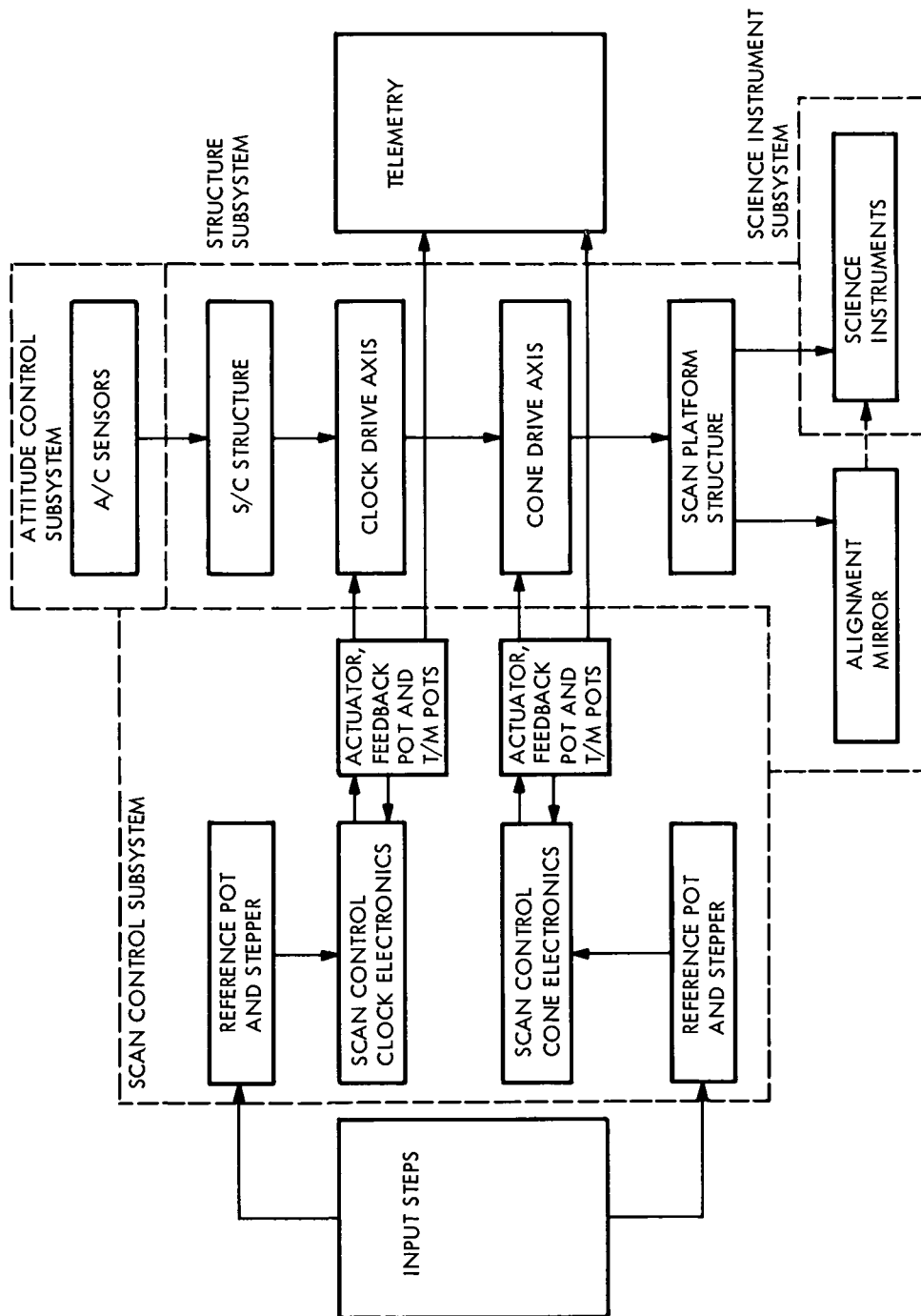


Figure 6 Scan Ground Calibration and Alignment Diagram

All telemetry calibrations with the exception of the scan fine positions were obtained by fitting output versus angle to a third order polynomial. The fine position required a more complicated calibration because of the gear train system driving the telemetry potentiometer. Undefined resistance regions occurred between maximum and minimum outputs as the pot completed a revolution every 4.5° . Center-to-center gear radius variations and gear ellipticity introduced additional errors.

To model these errors the fine position potentiometer output was assumed to be a third order polynomial in the potentiometer shaft angle (θ_P). θ_P is related to the actuator gimbal angle, θ_G , by

$$\theta_P = f_4 \left[\theta_G + \text{HAR}(\theta_G) \right] + n \cdot 360 \quad (7)$$

where all angles are in degrees

n is chosen to adjust θ_P to be between -180° and $+180^\circ$.

f_4 is the total gear ratio

HAR is the correction function for the gear train errors

$$\text{HAR}(\theta_G) = \sum_{i=1}^4 \left[H_{1i} \sin(f_i \theta_G) + H_{2i} (1 - \cos(f_i \theta_G)) + H_{3i} \sin(2f_i \theta_G) + H_{4i} (1 - \cos(2f_i \theta_G)) \right] \quad (8)$$

where H_{ji} , $j = 1$ to 4 , $i = 1$ to 4 , are the gear train errors.

$f_1 = 1.$, is the gear ratio from the gimbal axis to the first gear

$f_2 = f_1 \cdot \frac{84}{28} = 3$, is the gear ratio from the gimbal axis to the second gear.

$f_3 = f_2 \cdot \frac{113}{22} = 15.409091$, is the gear ratio from the gimbal axis to the fourth gear.

$f_4 = f_3 \cdot \frac{108}{21} = 79.246753$, is the gear ratio from the gimbal axis to the sixth gear or the potentiometer shaft.

The actuator gimbal angle, θ_G , is related to the clock and cone gimbal angles by

$$\alpha_G = \theta_G + 197.469^\circ \quad (9)$$

$$\beta_G = \theta_G + 101.042^\circ \quad (10)$$

The hysteresis error in the gear train was assumed random and is included in the accuracy of Table 1. During calibration two actuators exhibited high hysteresis and were interchanged with actuators with low hysteresis. No recalibration was necessary since the plan allowed for exchange of subsystem elements.

Subsequent in-flight calibration verified that the scan telemetry was within the calibration accuracy of Table 1. Sun sensor calibration was observed to have changed due to scale factor changes caused by decreasing solar intensity input and detector aging. A scale factor change of 20% yielded a maximum error of 0.05° at the edge of the 0.25° attitude control dead-band.

Control Loop Calibration

The control loop calibration was obtained from measurements on the reference and feedback potentiometers and scan control electronics. Data was obtained on the reference potentiometer by commanding a desired step position and measuring the required feedback to obtain an electrical null. The feedback data was obtained by moving the actuator gimbal axis reference to a known angle and measuring the feedback potentiometer output. The measurements were taken at equal potentiometer shaft angle increments of 8° . The feedback potentiometer output vs. actual gimbal angle (θ_G) and the required feedback for null vs. step position were fit to third order polynomials. The accuracy of the calibration is given in Table 2.

Table 2 Control Loop Potentiometer Calibration Accuracy

Potentiometer	3σ Accuracy, Degrees
Cone Reference	0.12
Clock Reference	0.26
Cone Feedback	0.17
Clock Feedback	0.34

The total 3σ accuracies for the control loops using the accuracies from Table 2 were 0.43° and 0.20° for the clock and cone axes, respectively. The clock axis calibration accuracy was not acceptable. However, when the control loops were integrated and tested, all errors were less than 0.20° , which led to the conclusion that a large part of the calibration error for the clock axis was due to errors in taking the measurements.

Later, testing on the PTM showed that the large calibration errors were real offsets. Therefore, the ground calibration control loop residuals were plotted as in Figure 7 to estimate corrections. The plotted corrections showed that an error of 0.25° was likely in the clock axis and updating by ground command was planned for in-flight calibration. Also, the in-flight calibration would provide a check of the estimated control loop corrections.

The differences between the measured gimbal angles from telemetry and the predicted gimbal angles from ground calibration provided the in-flight calibration of the control loop corrections. These corrections are also plotted in Figure 7. The ground and in-flight calibrations differ due to measurement error and interpolation error between data points. Subsequent analysis of potentiometer characteristics showed that the dominant error was the interpolation error and the ground calibration should have been performed at increments much less than the 8° used.

Electro-Mechanical Offsets

The ground calibration of the electro-mechanical offsets was obtained by measuring and combining numerous small rotation offsets. These offsets resulted from design limitations, manufacturing offsets, and assembly offsets. They are shown in Figures 8 and 9, and are related to the offset angles in the error model by Equations 11 through 18

$$\theta_1 = \delta_1 + \lambda - \sigma \quad (11)$$

$$\theta_2 = \delta_2 - \eta \quad (12)$$

$$\theta_3 = \delta_3 - \zeta \quad (13)$$

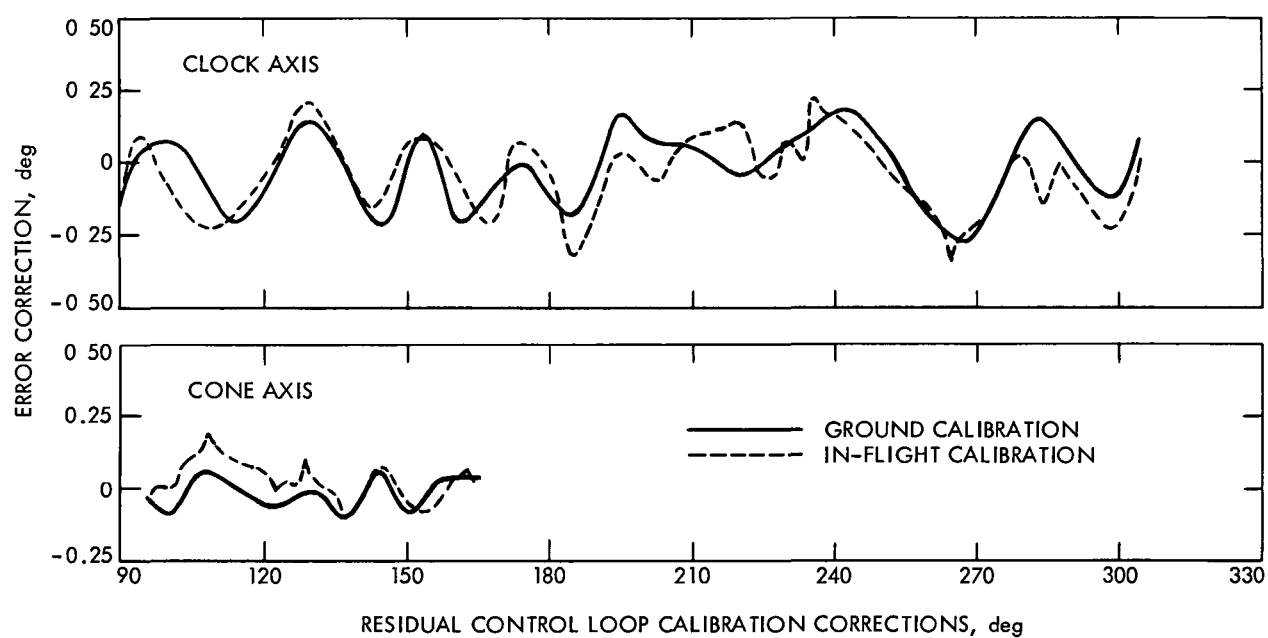


Figure 7. Control Loop Calibration Corrections

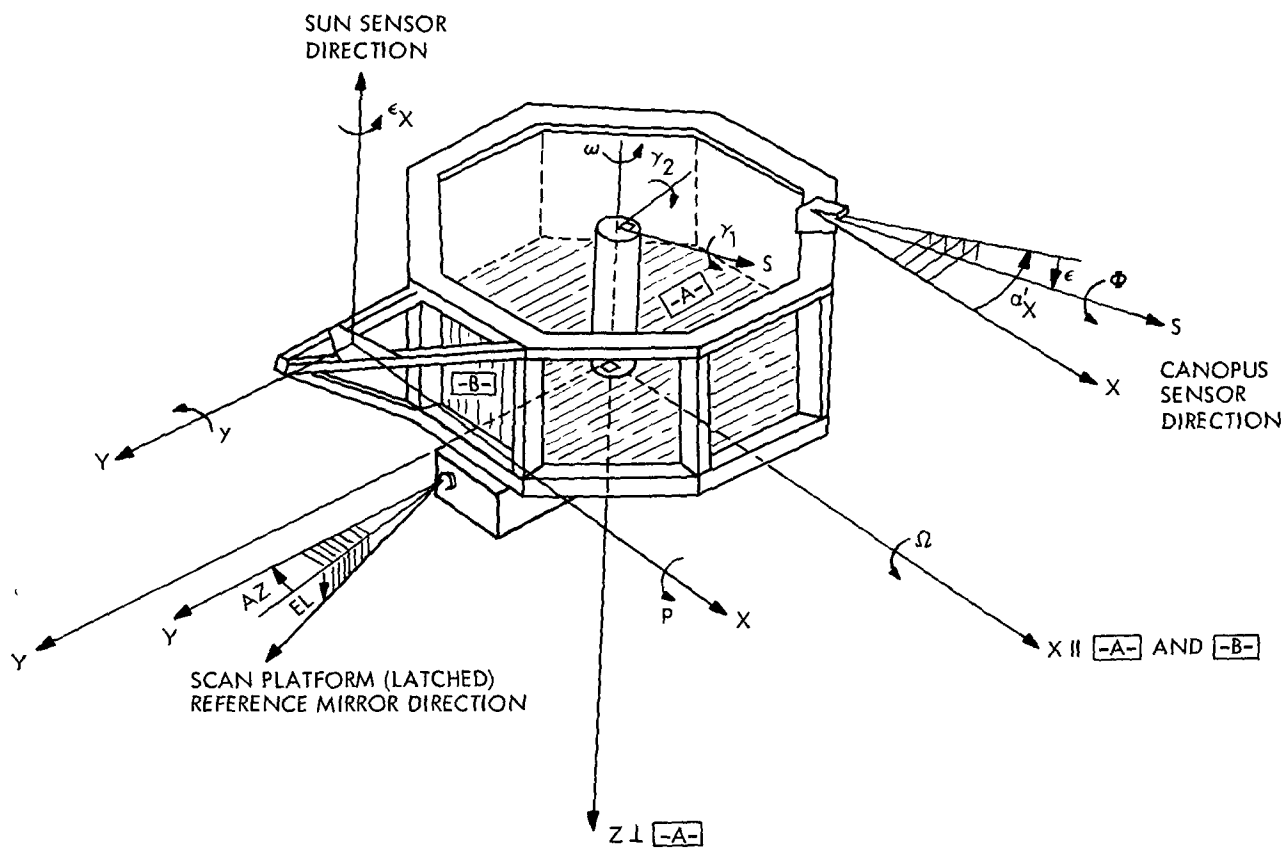


Figure 9 Spacecraft Offsets

$$\theta_4 = -\mu + \omega - \Delta + \epsilon_X - \alpha'_X + \alpha_X \quad (14)$$

$$\theta_5 = -\xi \quad (15)$$

$$\theta_6 = \gamma_1 + p \cos \alpha_X + y \sin \alpha_X \quad (16)$$

$$\theta_7 = \gamma_2 + p \sin \alpha_X - y \cos \alpha_X \quad (17)$$

$$\theta_8 = \Phi + p \cos \alpha_X + y \sin \alpha_X \quad (18)$$

The values for the offsets were obtained from Reference 5 and are summarized and defined in Table 3. The offset Δ is obtained from the Canopus tracker calibration and is a function of the Canopus cone angle. The fixed portion of this offset is shown in Table 3, and the residual dependence on cone angle is shown in Figure 10.

The results of combining the ground calibration measurements to obtain the angular offsets, θ_1 through θ_8 , are given in the Uncorrected column of Table 4. The angular offsets were to be corrected for the difference between the measured values of AZ and EL, and their expected values computed from scan telemetry of the latched position and the uncorrected offsets. The offsets were not corrected because the actuators were changed out, and no time was available for additional system testing. In-flight calibration showed that the latched position errors were mostly due to actuator zero reference angle errors. This can be demonstrated by correcting the offset θ_1 and θ_4 for the measured zero reference angle errors, -0.33° and -0.57° for the clock and cone actuators respectively and comparing the results to in-flight calibration. The results of the corrected calibration are given in the Corrected column of Table 4.

The accuracy of the ground calibration was determined from measurement accuracy of the error sources, expected changes of error sources due to aging or environmental conditions, and mechanical noise from bearing or gear backlash.

The accuracy in determining the latched position correction determined the accuracy of corrected values of θ_1 and θ_4 . The error in the latched position pointing was as large as 0.8° which determined the accuracy of the uncorrected values of θ_1 and θ_4 .

Table 3. Ground Calibration Offset Values

<u>Symbol</u>	<u>Description</u>	<u>Measured Value, Degrees</u>
μ	Clock actuator drive slot error.	0 0000
ξ	Nonorthogonality of the cone to clock drive axes.	-0 0723
σ	Cone actuator drive slot error.	0.0000
λ	Cone actuator case reference pin error.	0.0197
ζ	Cone drive axis offset from the platform in the M-N plane.	0.0000*
η	Cone drive axis offset from the platform in the L-N plane	0.0136
ω	Clock actuator case reference pin error	0 0000*
γ_1	Clock bearing tube offset from the Z-axis perpendicular to the Canopus sensor direction.	-0.0126
γ_2	Clock bearing tube offset from the Z-axis in the Canopus sensor direction	0 0127
Φ	Rotation error of the Canopus sensor.	0.0000
p	Pitch sun sensor null offset from the Z-axis (in the Y-axis direction)	-0.0208
y	Yaw sun sensor null offset from the Z-axis (in the minus X-axis direction).	0 0174
α_X^1	Measured clock angle of the X-axis	-32 1758
α_X	Designed clock angle of the X-axis	-32.2000*
ϵ	Cone offset of the Canopus sensor direction.	-0.0369
ϵ_X	Rotation error of the sun sensor.	0 0000
Ω	Nonorthogonality of the B-plane to the A-plane.	0 0027
EL	Reference mirror direction offset from the A-plane in the Z-axis direction	5 8875
AZ	Angle from the plane defined by the reference mirror direction and Z-axis to the Y-Z plane.	-0.0067
Δ	Canopus sensor roll offset from the Canopus tracker mounting reference	-0.0343
δ_1	TV-B look direction offset from the L-axis in M-axis direction	0 0425
δ_2	TV-B look direction offset from the L-axis in N-axis direction.	0 0625
δ_3	TV-B rotation offset around its look direction.	-0.0178

* Not measured.

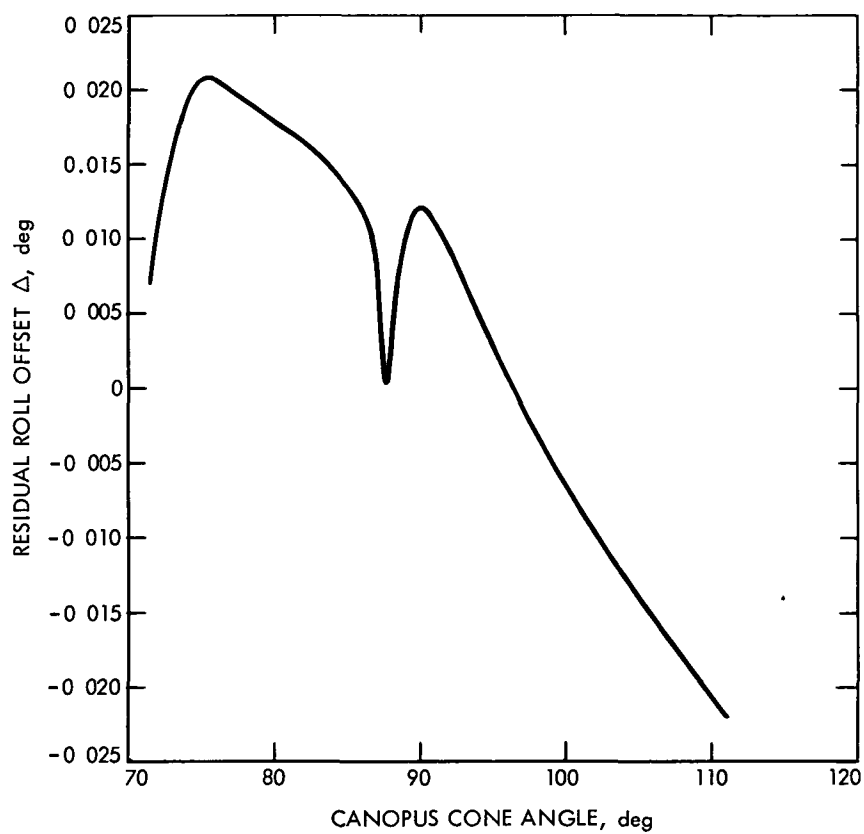


Figure 10. Residual Roll Null Offset

Table 4. Ground Calibration Results

Offset Symbol	Uncorrected		Corrected	
	Value (Deg)	3 σ Accuracy (Deg)	Value (Deg)	3 σ Accuracy (Deg)
θ_1	0.04250	0.6	-0.52800	0.3
θ_2	0.04889	0.04	0.04889	0.04
θ_3	-0.01778	0.1	-0.01778	0.1
θ_4	0.01143	0.6	-0.31900	0.3
θ_5	0.07231	0.2	0.07231	0.2
θ_6	0.00998	0.2	0.00998	0.2
θ_7	0.00770	0.2	0.00770	0.2
θ_8	0.02693	0.2	0.02693	0.2

The attitude control sun sensors were expected to change due to aging and changing solar intensity input. The aging effects were expected to be ninety percent completed in six weeks of flight and could introduce an electrical null offset of up to 0.1° . The increased sun sensor null offset uncertainty dominated the accuracy of offsets θ_6 , θ_7 , and θ_8 .

The mechanical noise affects the accuracy of all the offsets except θ_5 . For ground calibration the mechanical noise had a small effect on accuracy but limited the accuracy of in-flight calibration. The mechanical noise was demonstrated during in-flight calibration when the expected backlash range of 0.05° was observed in one star picture.

SECTION V

SCAN IN-FLIGHT CALIBRATION

To enhance the limited accuracy of the ground calibration, an in-flight calibration was performed prior to Mars encounter. The spacecraft-based measurements used in the in-flight calibration were the attitude control celestial sensor angles, scan platform gimbal angles and the television pictures from the science TV cameras. The attitude control celestial sensors measured the orientation of the spacecraft with respect to the sun and the star Canopus. The scan platform gimbals measured the orientation of the platform and television field-of-view with respect to the spacecraft. A TV picture of a known object provided the true pointing direction of the TV field-of-view. Stars were chosen primarily as calibration reference objects since their orientation relative to the spacecraft could be accurately determined.

The calibration was accomplished by calculating the expected image location of a star in a TV picture from trajectory data and attitude control and platform gimbal measurements. When compared to the observed TV star image location, an estimate of the pointing biases, equations (4) through (6), could be determined.

Data Processing

To provide sequence planning, facilitate data handling, and perform the estimation of the scan platform biases, an extensive computer software system was developed. It was comprised of six separate, but complementary, computer programs. Each program supplied some of the data which, when taken as a whole, provided the requisite calibration results. Software developed for the M'71 optical navigation demonstration (Reference 6) was utilized as much as practical to reduce development time and cost. Major functions of the software were the generating of data to facilitate the design of the calibration sequences and the processing of the telemetered data.

Planning Phase

In the planning and design phase, the desired pointing directions were determined. As indicated in Figure 11 the stars and planets to be used in the calibration sequences were selected by use of star atlases and the output of the Celestial Reference program (CELREF). CELREF (Ref. 7) provided position and visual magnitude data on stars observable in the field-of-view of the television cameras. The pointing directions for each picture were determined and verified by comparison of the output of the Celestial Geometry Generator (CGG) program with the star atlas data. CGG (Reference 8) combined spacecraft trajectory, star catalog and camera pointing data to compute a priori star image locations. Plotted output for each picture, scaled to match the hardcopy photographs, also assisted in locating and identifying the observed images. When a final set of desired pointing directions was determined, the Scan Platform Operations Program (SPOP) (Reference 9) was run to compute the number of commanded steps to the scan platform actuators to achieve the required pointing direction.

Processing Phase

As shown in Figure 11 both the science and the engineering telemetered data were processed to generate the required calibration results. The engineering telemetry tape E140 which contained the desired scan and attitude control limit cycle data was read by the Extractor program (XTR). XTR (Reference 10) computed the scan platform gimbal angles and the attitude reference angles. The scan platform gimbal angles were corrected to platform clock, cone and twist angles using linear corrections, equations (1) through (6), for the scan alignment parameters and the attitude control motion. The platform pointing error covariance matrix and angle variances were also determined and the results of these computations were punched on cards for use as part of the input to the Scan Calibration Program (SCALP).

As indicated in Figure 11 the platform clock, cone and twist angles and the shutter times of each picture were used by CGG to generate an overlay identifying the stars that were expected to be observed in the TV pictures. As part of the evaluation procedure hardcopy photos of the television pictures were

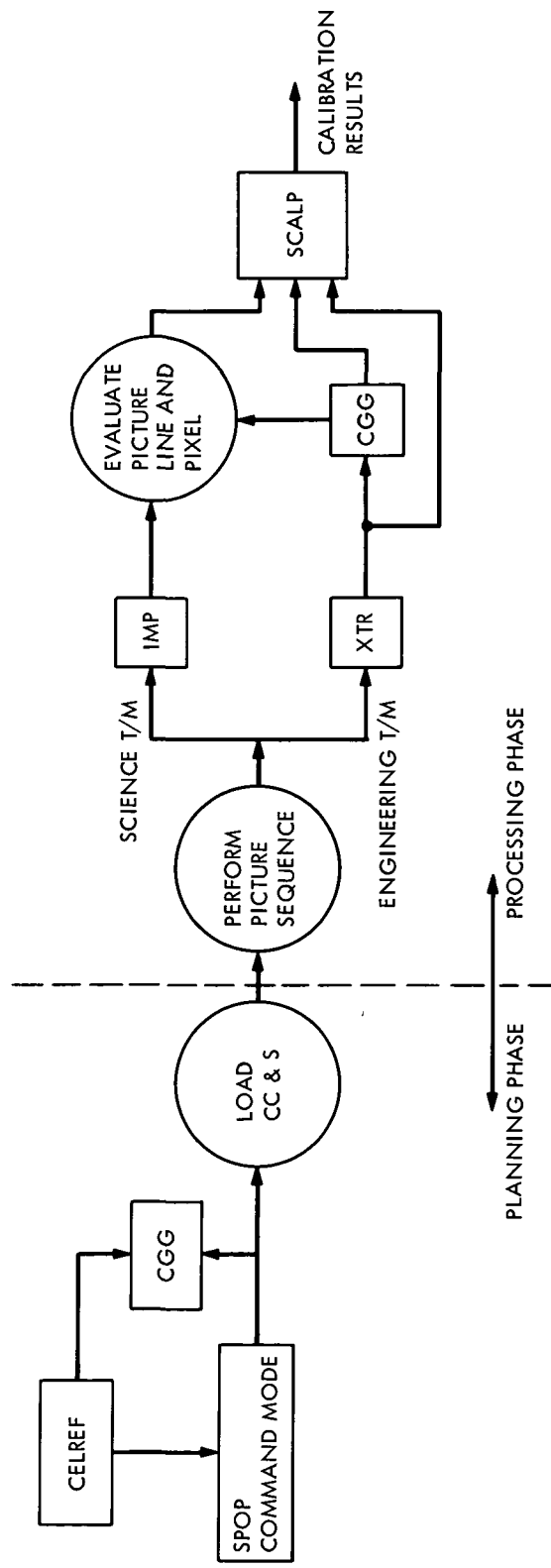


Figure 11. Scan In-Flight Calibration Software Data Flow

compared with the overlays to identify the star images seen therein. Figure 12 illustrates a typical CGG overlay and the TV picture to which it corresponds. The spacecraft-sun unit vector as determined by CGG was used as an input to SCALP.

Pictures of the stars and planets were obtained using the narrow angle science television camera, TV-B. The vidicon's active target raster was electronically scanned in 700 lines and sampled at 832 picture elements (pixels) per line. The 500 mm focal length lens resulted in a $1.1^\circ \times 1.4^\circ$ field-of-view with an angular resolution of 6 arc seconds. Each video sample was digitized to 9 bits (512 intensity levels) prior to transmission to earth. In order to accurately measure the location of star images on the TV picture an Image Processing program (IMP) was used to examine each picture in detail. IMP (Reference 11) generated both tabulated digital TV data as well as contour maps of each star image such as that shown in Figure 13. In this manner the precise center locations of the star, planet and resseau images contained in the telemetered video data could be determined to within ± 1 line and pixel after the images had been identified by use of the CGG overlays.

SCALP was adapted from the Optical Data Calibration and Rectification program (Reference 12) which was used in the M'71 optical navigation demonstration. The input to SCALP for each picture consisted of the scan platform gimbal angles, the limit cycle angles, the spacecraft-sun unit vector, the image locations in the picture and the celestial coordinates of the images. SCALP combined these data with the spacecraft and TV error models to calculate expected image position, image position partial derivatives with respect to error parameters and trajectory vectors, and the pointing error covariance matrix. Uncertainties in selected error parameters were estimated from the observed and calculated image positions in the TV pictures. The TV picture pointing errors and the a posteriori residuals were also determined.

Calibration Sequences

The in-flight calibration plan called for two sequences of TV pictures. The first sequence, Scan Calibration I (Scan I), was designed to determine the gross biases in the platform pointing system. This sequence involved taking groups of

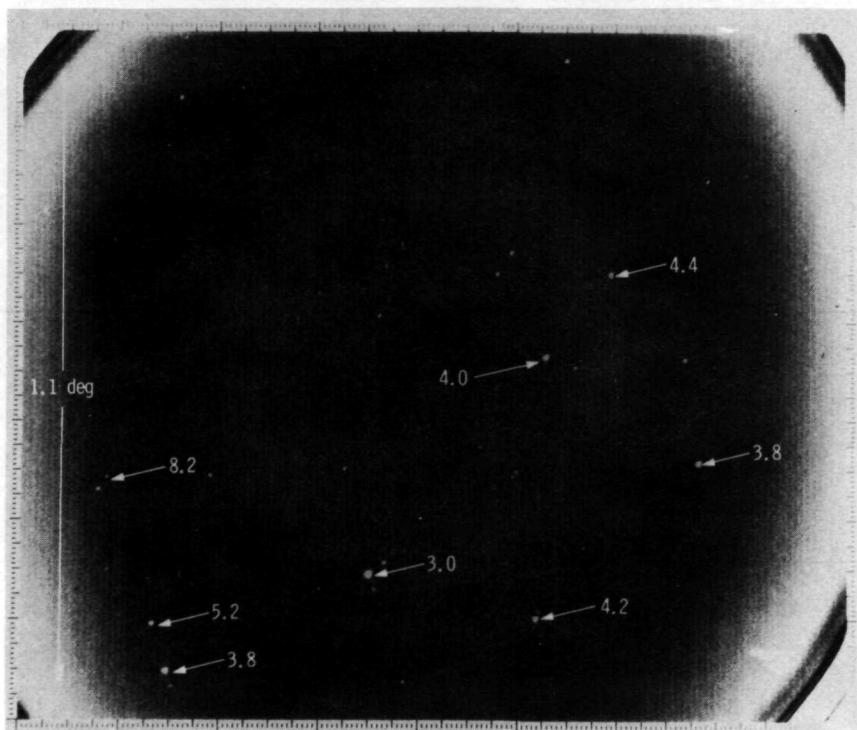
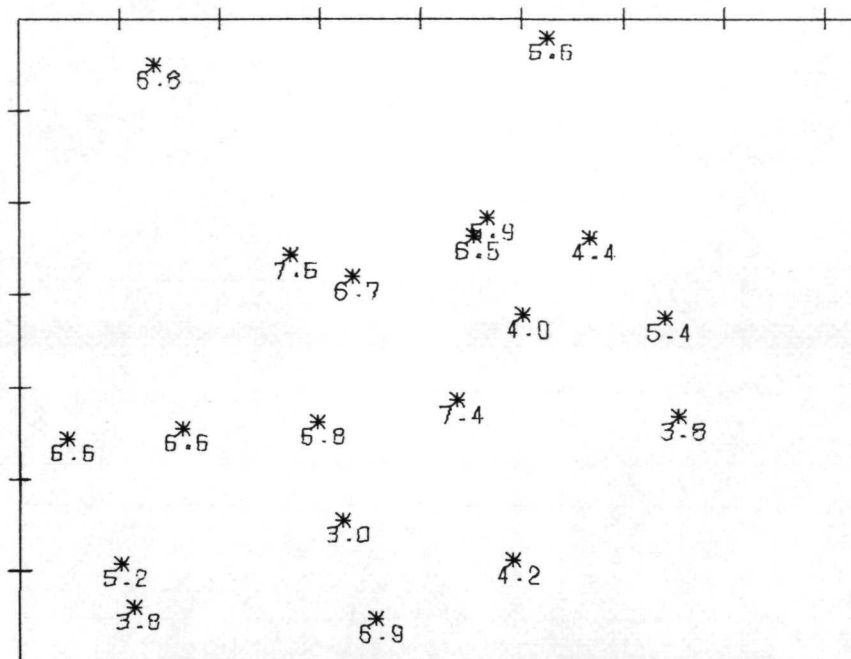


Figure 12. Simulated and Actual TV Star Picture

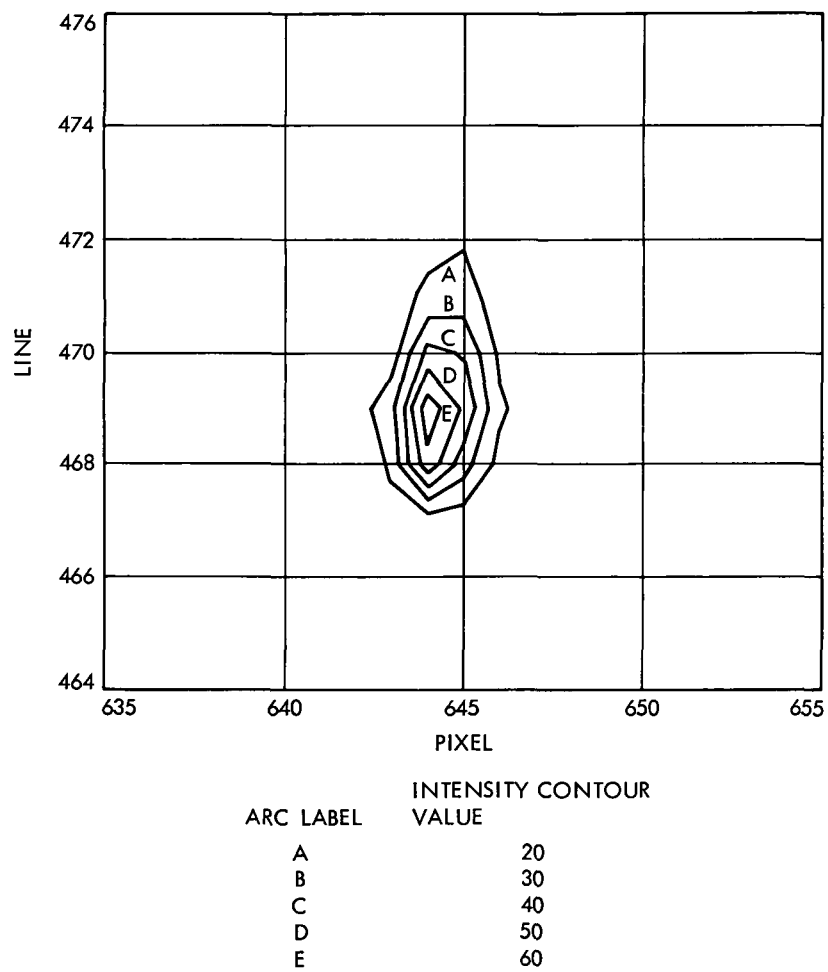


Figure 13. Video Contour Plot of 6.9 Magnitude Star

pictures of stars in patterns to maximize probability of obtaining star picture data. The second calibration sequence, Scan Calibration II (Scan II), was designed to determine platform pointing offsets over the entire dynamic range of scan platform motion.

Scan Calibration I

Scan I was performed October 2, 1971, 43 days before Mars encounter. Considerable planning went into the calibration both in terms of actual sequence development and in working the data processing interfaces to be exercised following the calibration. The sequence was tested on the PTM six weeks prior to Scan I to obtain an end to end check from platform slews through final calibration.

Thirty TV pictures were taken during Scan I, of which eighteen were budgeted to scan pointing recalibration and twelve to TV engineering. The calibration plan called for three clusters of six pictures centered on bright stars. Of the six pictures, the second was from the $11^\circ \times 14^\circ$ wide angle camera, TV-A, and five were from the narrow angle camera, TV-B, taken in a cross-shaped search pattern illustrated in Figure 14. This pattern maximized the probability of obtaining a star in one or more of the TV-B pictures for the expected pointing accuracy of 0.8° (Reference 13). The one TV-A picture assured obtaining star data even if no data were obtained in the TV-B pictures.

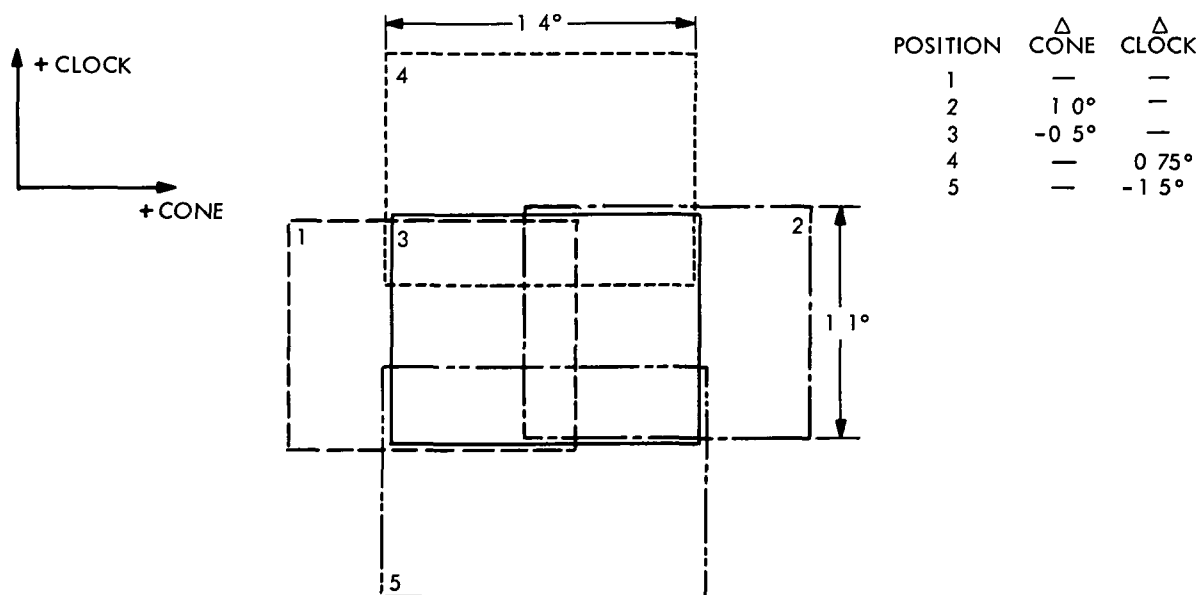


Figure 14. Search Pattern for Scan I

The three targets chosen as bright enough for TV-A were stars Vega (α Lyra), Altair (α Aquila) and Aldebaran (α Taurus). The sequence of Scan I pictures and their respective pointing directions are given in Appendix A and Reference 14

The remaining twelve pictures were taken for TV-B photometric calibration. Data from these pictures were included in the scan pointing calibration. The first two of these pictures were of Saturn, taken 84 seconds apart at the same platform gimbals position. The last ten pictures were taken of the Pleiades. Five pairs of TV-B pictures were taken in the pattern illustrated in Figure 15. This pattern was used to maximize both the coverage of the Pleiades and the probability that some bright stars would be photographed even if pointing offsets were large

The sequence of slewing and picture-taking was under control of the CC&S. Allowances were made for compensation of the control loop errors by ground command. During the long slews between target stars, control loop non-linearities, Figure 7, could introduce errors on the order of 0.25° . A ground command was sent to initiate each picture sequence after its initial position was checked. Twice in Scan I a QC was sent to correct the initial pointing of a picture sequence.

POSITION	Δ CONE	Δ CLOCK
1	—	—
2	-0.5°	—
3	-0.25°	0.5°
4	0.5°	—
5	0.5°	—

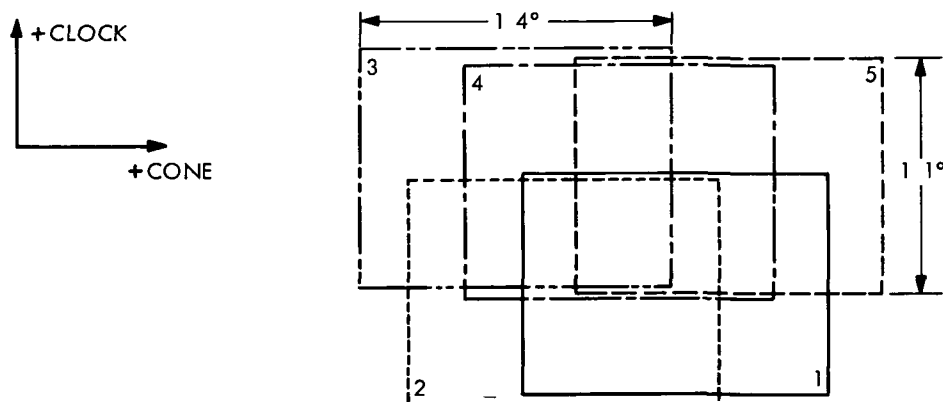


Figure 15 Search Pattern for Pleiades Pictures

Immediately following the recording of the last TV picture, the 3-1/2 hour playback of the thirty Scan I pictures began. Identifiable stars were observed in all 30 pictures. TV-B sensitivity was much better than expected, and scan pointing offsets were well within the planned tolerances. The systematic data reduction which began with the return of the first real time engineering data continued for 24 hours until the first estimation of the scan platform pointing biases was obtained. This was used to plan Scan II whose final input was due 2-1/2 days following Scan I.

Scan Calibration II

Scan II was performed October 8, 1971, six days following Scan I. The sequence, including the playback of the pictures, was executed in seventeen hours.

Scan II was planned to determine platform pointing offsets over the entire range of scan platform motion. This was to be accomplished by taking thirty TV-B pictures distributed over the complete platform FOV. Scan II was initially planned to be independent of Scan I and thus necessarily operative without knowledge of the large unknown offsets (and TV photometric sensitivity) to be determined from Scan I. This was the plan because of the large amount of processing necessary to reduce Scan I data and the short time between Scan I and Scan II. However, Scan I data were reduced in a timely manner for use in Scan II planning. Achievement of the initial recalibration of the platform pointing system and the excellent vidicon sensitivity observed in the first set of pictures permitted some retargeting to optimize the second calibration sequence.

Thirty TV-B pictures were taken of 30 separate targets distributed over the entire platform field of view. A star map showing the target stars and the pattern of slews between them is given in Figure 16. A list of the 30 targets is given in Appendix B.

As in Scan I the sequence of slewing, picture shuttering and recording was under control of the CC&S except that a ground command was required to set a computer internal flag prior to each picture. This flexibility turned out to be

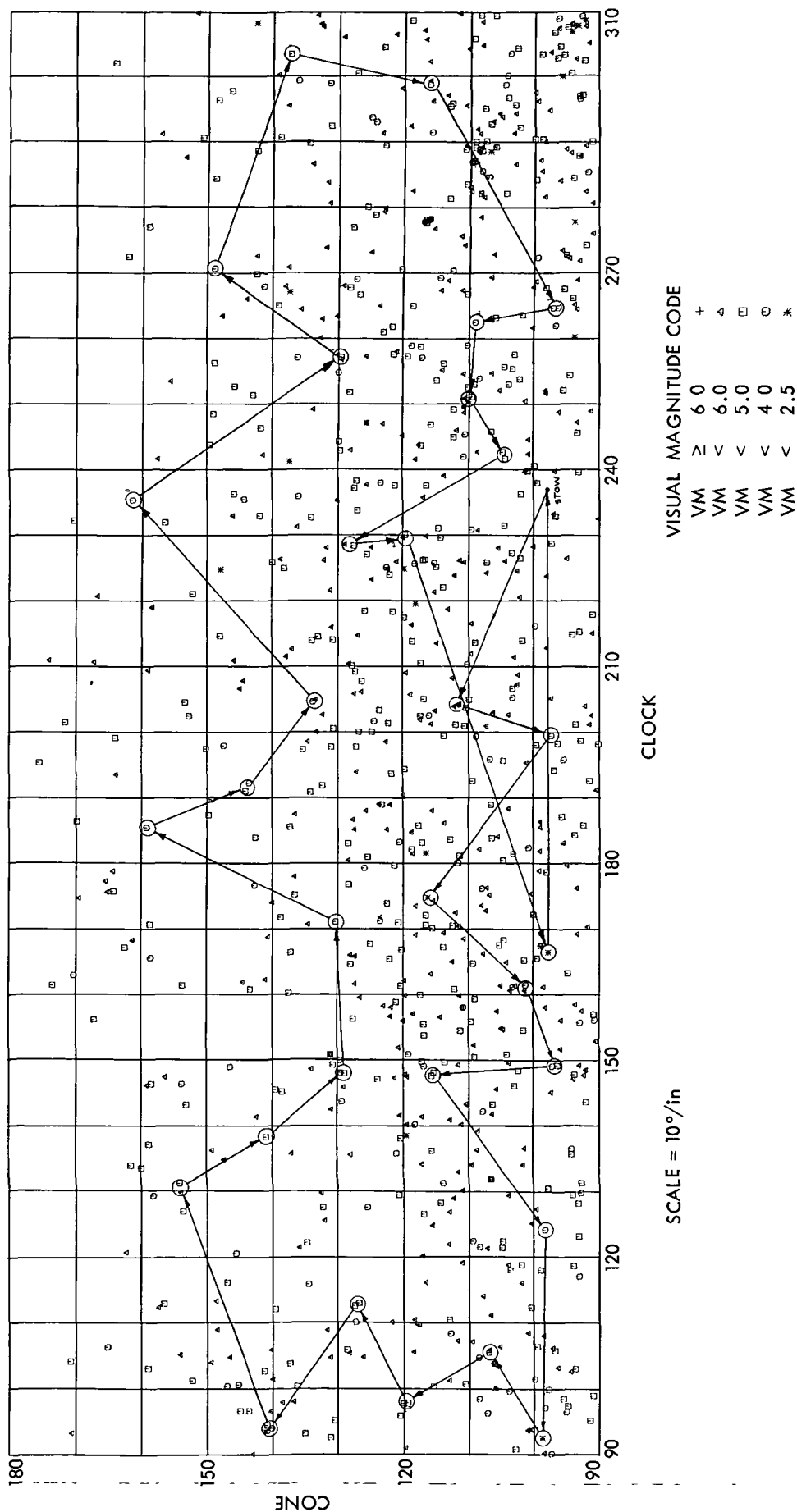


Figure 16 Scan II Sequence

very useful as the sequence was modified in real time to optimize pointing prior to many pictures. This was necessary for three reasons. First, CC&S loading problems necessitated the delay of Scan II execution for 24 hours. This delay in turn required the hasty update of the pointing of the pictures to account for the spacecraft's 0.5° motion around the sun in 24 hours. The update could not be optimized on short notice and hence QCs were needed in real time to correct pointing. Second, the platform control loop errors necessitated much more compensation in Scan II because of the many long slews. Third, to accommodate some Ultraviolet Spectrometer pointing calibration requests, a number of QCs were added near the end of the sequence. A total of 28 QCs were sent in the course of Scan II. They are detailed in the preliminary report, Reference 15.

SECTION VI

RESULTS AND CONCLUSIONS

The change in the angular offsets resulting from the in-flight calibration is shown in Table 5. The values obtained during ground calibration are repeated for comparison.

Table 5. In-Flight Calibration Results

Angular Offset	Ground Calibration Degrees	In-Flight Calibration Degrees
θ_1	0.04250	-0.47719
θ_2	0.04889	0.15438
θ_3	-0.01778	0.13924
θ_4	0.01143	-0.28496
θ_5	0.07231	-0.12845
θ_6	0.00998	0.08978
θ_7	0.00770	0.12057
θ_8	0.02693	-0.17170

Table 6 shows the summary of the accuracies obtained from Scan I and II as detailed in Appendices A and B. Mission requirements were met after Scan II.

After Scan II additional processing (Reference 16) was performed to include new estimates of the sun sensors' scale factors and add an additional harmonic term to the clock axis telemetry calibration. This reduced pointing knowledge uncertainty to 0.05° (3σ) per axis.

Table 6. Scan Pointing Accuracy

	Mission Requirements 3 σ Degrees/Axis	Post Scan I 3 σ Degrees (Cone Cross-Cone)	Post Scan II 3 σ Degrees (Cone Cross-Cone)
Pointing Control	0.5°	0.570 0.622	0.486 0.378
Pointing Knowledge	0.25°	0.153 0.090	0.153 0.096

Based on results of the ground and in-flight calibrations, the following conclusions can be drawn.

1. Additional control loop calibration should be performed during ground testing. Non-linearities in potentiometers contributed to large interpolation errors. These errors could be greatly reduced by taking a finer grid of data.
2. Accurate telemetry calibration should be obtained during ground testing. Considerable effort was expended modeling gear train harmonics with a resulting high accuracy. This data would have been difficult to obtain with only an in-flight calibration.
3. The plan for obtaining electro-mechanical offsets was good. Switching the actuators at the last minute and lack of time resulted in not using data which was good. With care ground calibration should yield overall accuracies of 0.1° to 0.2° (3 σ).
4. On the other hand, if an in-flight calibration is guaranteed, no ground calibration of electro-mechanical offsets is required. As-built tolerances provide an accuracy sufficient for a starting point for in-flight calibration.
5. At least two in-flight calibrations are required. Pointing knowledge can be sufficiently determined with one calibration, but a second calibration is required to assure meeting pointing control requirements.
6. The two in-flight calibrations should be at least a week apart to allow for data reduction and planning.
7. Testing the first in-flight sequence with the PTM was a valuable aid.

8. In-flight calibration reduced the pointing control error to the uncertainties caused by platform step size and attitude control dead-band.
9. In-flight calibration can reduce the pointing knowledge error to the resolution of the telemetry. Another calibration spaced several months after Scan II would indicate the stability of this calibration by estimating scale factor changes and other drifts.
10. The in-flight calibration technique is a valuable aid and can be used in the future when imaging experiments are flown.

APPENDIX A

RESULTS OF SCAN I

The following is a tabulation of the data obtained during the first scan calibration sequence.

Included in this table are:

1. Desired pointing angles (clock and cone) for each picture.
2. Pointing angles obtained based on scan platform and attitude control engineering telemetry.
3. Pointing angles obtained based on observed star images
4. Pointing control accuracy (3 - 1).
5. Pointing knowledge accuracy (2 - 3).
6. Statistics associated with pointing control and knowledge accuracy.

SCAN I

Picture No	1 Desired Angles (Clock) (Cone)	2 Angles Obtained From Eng. T/M (Clock) (Cone)	3 Angles Obtained From Star Images (Clock) (Cone)	4 Control Accuracy (3-1) (Cross-Cone) (Cone)	5 Inertial Knowledge Accuracy (2-3) (Cross-Cone) (Cone)
1	166.83 98.88	166.455 98 122	166.502 98 201	-0.324 -0.679	-0.046 -0 079
2	166 83 98 88	166 005 97 981	166 006 98.018	-0.814 -0.862	-0.001 -0.037
3	166.83 99 88	166.504 99.061	166.559 99 154	-0 268 -0.726	-0.054 -0.093
4	166 83 99 38	166.596 98 625	166.621 98 685	-0.206 -0.695	-0.025 -0.060
5	167.58 99 38	167 342 98 652	167.407 98.704	-0 171 -0 676	-0.064 -0.052
6	166 08 99 38	165.939 98 678	165.977 98.729	-0.102 -0 651	-0.038 -0.051
7	139.49 122 55	139.322 121 898	139 342 121 793	-0.124 -0.757	-0.017 0.105
8	139.49 122.55	138 816 121.736	138 784 121.687	-0 595 -0 863	0.027 0 049
9	139 49 123.55	139 363 122 766	139 377 122.779	-0 094 -0.771	-0 012 -0 013
10	139 49 123 05	139 271 122 384	139 293 122.365	-0.165 -0 685	-0.018 0.019
11	140.24 123 05	139.930 122.364	139.928 122.294	-0 262 -0.756	0 002 0.070
12	138.74 123 05	138 423 122 331	138 442 122 262	-0 250 -0.788	-0.016 0 069
13	288 85 104 31	288.429 103 733	288 429 103.733	-0.408 -0.577	0 0
14	288.85 104.31	287.976 103.597	287 988 103.599	-0 835 -0.711	-0.012 -0 002
15	288.85 105.31	288 509 104 667	288.508 104 778	-0 330 -0.532	0.001 -0 111
16	288.85 104 81	288.602 104 279	288.591 104 304	-0.250 -0 506	0.011 -0.025

SCAN I

Picture No.	1 Desired Angles (Clock) (Cone)	2 Angles Obtained From Eng. T/M (Clock) (Cone)	3 Angles Obtained From Star Images (Clock) (Cone)	4 Control Accuracy (3-1) (Cross-Cone) (Cone)	5 Inertial Knowledge Accuracy (2-3) (Cross-Cone) (Cone)
17	289.60 104.81	289.358 104.302	289.362 104.328	-0.230 -0.482	-0.004 -0.026
18	288.10 104.81	287.920 104.319	287.941 104.323	-0.154 -0.487	-0.020 -0.004
19	284.77 103.24	284.336 102.909	284.302 102.913	-0.456 -0.327	0.033 -0.004
20	284.77 103.24	284.435 102.867	284.383 102.876	-0.377 -0.364	0.051 -0.009
21	277.90 112.90	277.488 112.533	277.517 122.491	-0.353 -0.409	-0.027 0.042
22	277.90 112.90	277.483 112.500	277.511 112.469	-0.358 -0.431	-0.026 0.031
23	277.90 112.40	277.588 111.977	277.595 111.972	-0.282 -0.428	-0.007 0.005
24	277.90 112.40	277.608 112.025	277.624 112.010	-0.255 -0.390	-0.015 0.015
25	278.40 112.15	277.626 111.900	277.568 111.829	-0.771 -0.321	0.054 0.071
26	278.40 112.15	277.633 111.870	277.582 111.805	-0.758 -0.345	0.047 0.065
27	278.40 112.65	278.103 112.425	278.063 112.438	-0.311 -0.212	0.037 -0.013
28	278.40 112.65	278.129 112.382	278.090 112.412	-0.286 -0.238	0.036 -0.030
29	278.40 113.15	277.840 112.749	277.856 112.737	-0.500 -0.413	-0.015 0.012
30	278.40 113.15	277.878 112.766	277.883 112.747	-0.475 -0.403	-0.005 0.019
			6 μ	-0.359	-0.004
			μ	-0.550	-0.001
			σ	0.209	0.030
			σ	0.190	0.051

APPENDIX B

RESULTS OF SCAN II

The following is a tabulation of the data obtained during the second scan calibration sequence. The data contained herein is in a format similar to that presented in Appendix A.

SCAN II

Picture No	1 Desired Angles (Clock) (Cone)	2 Angles Obtained From Eng T/M (Clock) (Cone)	3 Angles Obtained From Star Images (Clock) (Cone)	4 Control Accuracy (3-1) (Cross-Cone) (Cone)	5 Inertial Knowledge Accuracy (2-3) (Cross-Cone) (Cone)
1	204 01 112 03	204 079 112 367	204 146 112 358	0 126 0 328	-0 062 0 009
2	199 97 97 64	199 753 97 328	199 817 97 409	-0 152 -0.191	-0 064 -0 081
3	174 69 115 93	174 518 115 873	174 564 115 891	-0 113 -0 039	-0 041 -0 018
4	161 13 103 02	160 925 103 084	160 974 103 010	-0 152 -0 010	-0 048 0 074
5	149.23 96 43	149.339 96 451	149.353 96 488	0.122 0 018	-0.014 -0 037
6	147 81 115 20	147 525 115 445	147 554 115 400	-0.232 0 200	-0 026 0 045
7	124 29 97 78	124 417 98 063	124 436 98 047	0.145 0 187	-0 019 0 016
8	92 58 98 34	92 930 98 216	92 939 98 239	0 236 -0 101	-0 009 -0 023
9	105 89 106 09	105 681 106 317	105 702 106 234	-0 181 0 144	-0 020 0 083
10	98 00 119 08	97 766 118 700	97 792 118 663	-0 182 -0 217	-0 022 0 037
11	113 17 126 29	113 127 126 071	113 139 126 018	-0 025 -0 052	-0 010 0 053
12	93 67 140 29	93 866 140 430	93 878 140 343	0 133 0 053	-0 008 0 087
13	130 02 153 64	129 696 153 658	129 696 153 578	-0 144 -0 062	0 0 080
14	137 86 140.52	137 977 140 263	137 923 140.269	0 040 -0 251	0 034 -0 006
15	147 89 129 16	147 845 129 048	147 870 129 068	-0 016 0 018	-0 020 -0 020
16	170 71 130 09	170 673 130 300	170 699 130 252	-0 008 0 162	-0 020 0 048

SCAN II

Picture No	1 Desired Angles (Clock) (Cone)	2 Angles Obtained From Eng T/M (Clock) (Cone)	3 Angles Obtained From Star Images (Clock) (Cone)	4 Control Accuracy (3-1) (Cross-Cone) (Cone)	5 Inertial Knowledge Accuracy (Cross-Cone) (Cone)
17	184 58 159 29	184 307 159 608	184 292 159 568	0 102 0 278	0 005 0 040
18	191 26 143.98	191 093 143.810	191 095 143.895	-0.061 -0.085	-0.001 -0.085
19	204.57 133 82	204 790 134 168	204.805 134.113	0.170 0.293	-0.011 0.055
20	234.41 161.63	234.248 161 533	234.237 161.576	-0.054 -0.054	0.003 -0 043
21	257.56 130.05	257 802 130.255	257 736 130.220	0.135 0.170	0.050 0.035
22	271 16 149.75	270.772 149.651	270.842 149.635	-0.160 -0.115	-0.035 0.016
23	303.90 137.90	304 155 137.666	304 088 137 652	0.126 -0.248	0.045 0.014
24	299 36 116 51	299.337 116 391	299 306 116.418	-0.048 -0.002	0.028 -0.027
25	265 12 97.31	264 983 97 034	264.974 97.095	-0 145 -0 215	0.009 -0.061
26	263 10 109.38	263 111 109.459	263 087 109.458	-0.012 -0.078	0 022 0.001
27	250.77 110 29	250.887 110.403	250 904 110.443	0.126 0 153	-0.016 -0.040
28	241 78 104 59	241 805 104.667	241 846 104.722	0.064 0.132	-0.040 -0.055
29	228.32 128 28	228.284 128.523	228.338 128.489	0 014 0.209	-0.042 0.034
30	219.46 118.46	219.361 118.363	219.460 118 425	0 -0.035	-0 087 -0.062
31	166.44 97.53	166 387 97 367	166.402 97 431	-0.038 -0.099	-0.015 -0.064
			6 μ	-0.006	-0.013
			μ	0 014	0.003
			σ	0 126	0.032
			σ	-0.162	-0.051

REFERENCES

1. Havens, W. F., Preska, D. C., Virzi, R. A., "Mariner Mars 1971 Guidance and Control System Functional Description and Block Diagram," Project Document 610-145, Jet Propulsion Laboratory, Pasadena, California.
2. "Scan Calibration Plan," in Flight Projects, Space Programs Summary 37-61, Vol. I, pp. 12-14, Jet Propulsion Laboratory, Pasadena, California, Jan 31, 1970.
3. "Mariner Mars 1971 Scan Platform Control Calibration and Alignment Plan," Project Document 610-126, Jet Propulsion Laboratory, Pasadena, California, June 18, 1970.
4. "Mariner Mars 71-2 Telemetry Calibration Curves," Project Document 610-156, Jet Propulsion Laboratory, Pasadena, California. April 14, 1971.
5. Coyle, G., et al., "MM '72 Octagon and Scan Platform Mechanical Alignment - Final Issue," Interoffice Memorandum, Jet Propulsion Laboratory, Pasadena, California, Jan. 19, 1971.
6. Acton, C. H., "Processing On-Board Optical Data for Planetary Approach Navigation," AIAA Paper 72-53, presented at the AIAA 10th Aerospace Sciences Meeting, San Diego, California, Jan. 17-19, 1972.
7. "Celestial Reference Program User's Manual," Report 900-503, Jet Propulsion Laboratory, Pasadena, California, Sept 28, 1971.
8. "Optical Navigation Demonstration Programmer's Reference Manual," Vol. VI, CGG, Celestial Geometry Generator, Report 900-468, Jet Propulsion Laboratory, Pasadena, California, June 30, 1971
9. "Scan Platform Operations Program Command Mode User's Guide," TR-72-1306-329-2, Informatics Inc., Canoga Park, California, Feb. 15, 1972.
10. "Optical Navigation Demonstration Programmer's Reference Manual," Vol. V, XTR, Extractor Program, Report 900-467, Jet Propulsion Laboratory, Pasadena, California, Sept. 10, 1971.
11. "Optical Navigation Demonstration Programmer's Reference Manual," Vol. VII, IMP, Image Processing Program, Report 900-469, Jet Propulsion Laboratory, Pasadena, California, June 30, 1971.
12. "Optical Navigation Demonstration Programmer's Reference Manual," Vol. VIII, ODCR, Optical Data Calibration and Rectification Program, Report 900-470, Jet Propulsion Laboratory, Pasadena, California, June 30, 1971.

REFERENCES (contd)

13. Virzi, R. A. , "Scan Calibration Search Pattern Sequence," Interoffice Memorandum 343-5-71-126, Jet Propulsion Laboratory, Pasadena, California, March 1, 1971
14. Havens, W F , "Finalized Input for Scan Calibration I," Interoffice Memorandum 343-5-71-592, Jet Propulsion Laboratory, Pasadena, California, Sept. 27, 1971.
15. Havens, W. F. , "Preliminary Engineering Values and Calibration Results from Scan Calibrations, Interoffice Memorandum 343-5-71-668, Jet Propulsion Laboratory, Pasadena, California, Oct 25, 1971
16. Acton, C. H. , and Duxbury, T C , "On-Board Optical Navigation Data from MM '71," Institute of Navigation, National Space Meeting, Orlando, Florida, March 15-16, 1972.

1. Report No. 33-556	2. Government Accession No.	3. Recipient's Catalog No.	
4. Title and Subtitle SCAN POINTING CALIBRATION FOR THE MARINER MARS 1971 SPACECRAFT		5. Report Date August 1, 1972	
		6. Performing Organization Code	
7. Author(s) W. F. Havens, G. I. Jaivin, G. D. Pace, R. A. Virzi		8. Performing Organization Report No.	
9. Performing Organization Name and Address JET PROPULSION LABORATORY California Institute of Technology 4800 Oak Grove Drive Pasadena, California 91103		10. Work Unit No.	
		11. Contract or Grant No. NAS 7-100	
		13. Type of Report and Period Covered Technical Memorandum	
12. Sponsoring Agency Name and Address NATIONAL AERONAUTICS AND SPACE ADMINISTRATION Washington, D.C. 20546		14. Sponsoring Agency Code	
15. Supplementary Notes			
16. Abstract The methods used to calibrate the pointing direction of the M'71 spacecraft scan platform are described here. Accurate calibration was required to meet the pointing accuracy requirements of the scientific instruments mounted on the platform. A detailed ground calibration was combined with an in-flight calibration utilizing narrow angle television pictures of stars. Results of these calibrations are summarized.			
17. Key Words (Selected by Author(s)) Control and Guidance Mariner Mars 1971 Project		18. Distribution Statement Unclassified -- Unlimited	
19. Security Classif. (of this report) Unclassified	20. Security Classif. (of this page) Unclassified	21. No. of Pages 42	22. Price

HOW TO FILL OUT THE TECHNICAL REPORT STANDARD TITLE PAGE

Make items 1, 4, 5, 9, 12, and 13 agree with the corresponding information on the report cover. Use all capital letters for title (item 4). Leave items 2, 6, and 14 blank. Complete the remaining items as follows:

3. Recipient's Catalog No. Reserved for use by report recipients.
7. Author(s). Include corresponding information from the report cover. In addition, list the affiliation of an author if it differs from that of the performing organization.
8. Performing Organization Report No. Insert if performing organization wishes to assign this number.
10. Work Unit No. Use the agency-wide code (for example, 923-50-10-06-72), which uniquely identifies the work unit under which the work was authorized. Non-NASA performing organizations will leave this blank.
11. Insert the number of the contract or grant under which the report was prepared.
15. Supplementary Notes. Enter information not included elsewhere but useful, such as: Prepared in cooperation with... Translation of (or by)... Presented at conference of... To be published in...
16. Abstract. Include a brief (not to exceed 200 words) factual summary of the most significant information contained in the report. If possible, the abstract of a classified report should be unclassified. If the report contains a significant bibliography or literature survey, mention it here.
17. Key Words. Insert terms or short phrases selected by the author that identify the principal subjects covered in the report, and that are sufficiently specific and precise to be used for cataloging.
18. Distribution Statement. Enter one of the authorized statements used to denote releasability to the public or a limitation on dissemination for reasons other than security of defense information. Authorized statements are "Unclassified-Unlimited," "U. S. Government and Contractors only," "U. S. Government Agencies only," and "NASA and NASA Contractors only."
19. Security Classification (of report). NOTE: Reports carrying a security classification will require additional markings giving security and downgrading information as specified by the Security Requirements Checklist and the DoD Industrial Security Manual (DoD 5220.22-M).
20. Security Classification (of this page). NOTE: Because this page may be used in preparing announcements, bibliographies, and data banks, it should be unclassified if possible. If a classification is required, indicate separately the classification of the title and the abstract by following these items with either "(U)" for unclassified, or "(C)" or "(S)" as applicable for classified items.
21. No. of Pages. Insert the number of pages.
22. Price. Insert the price set by the Clearinghouse for Federal Scientific and Technical Information or the Government Printing Office, if known.